Article

Protein Surface-Assisted Enhancement in the Binding Affinity of an Inhibitor for Recombinant Human Carbonic Anhydrase-II

Abir L. Banerjee, Michael Swanson, Bidhan C. Roy, Xiao Jia, Manas K. Haldar, Sanku Mallik, and D. K. Srivastava

More About This Article

Additional resources and features associated with this article are available within the HTML version:

- Supporting Information
- Links to the 2 articles that cite this article, as of the time of this article download
- Access to high resolution figures
- Links to articles and content related to this article
- Copyright permission to reproduce figures and/or text from this article

View the Full Text HTML

Protein Surface-Assisted Enhancement in the Binding Affinity of an Inhibitor for Recombinant Human Carbonic Anhydrase-II

Abir L. Banerjee, Michael Swanson, Bidhan C. Roy, Xiao Jia, Manas K. Haldar, Sanku Mallik,* and D. K. Srivastava*

Contribution from the Department of Chemistry and Molecular Biology, North Dakota State University, Fargo, North Dakota 58105

Received April 27, 2004; E-mail: dk.srivastava@ndsu.nodak.edu; sanku.mallik@ndsu.nodak.edu

Abstract: We elaborate on a novel strategy for enhancing the binding affinity of an active-site directed inhibitor by attaching a tether group, designed to interact with the surface-exposed histidine residue(s) of enzymes. In this approach, we have utilized the recombinant form of human carbonic anhydrase-II (hCA-II) as the enzyme source and benzenesulfonamide and its derivatives as inhibitors. The steady-state kinetic and the ligand binding data revealed that the attachment of iminodiacetate (IDA)-Cu^{2+} to benzenesulfonamide (via a triethylene glycol spacer) enhanced its binding affinity for hCA-II by about 40-fold. No energetic contribution of either IDA or triethylene glycol spacer was found (at least in the ground state of the enzyme—inhibitor complex) when Cu^{2+} was stripped off from the tether group-conjugated sulfonamide derivative. Arguments are presented that the overall strategy of enhancing the binding affinities of known inhibitors by attaching the IDA-Cu^{2+} groups to interact with the surface-exposed histidine residues will find a general application in designing the isozyme-specific inhibitors as potential drugs.

Introduction

Following the completion of the human genome project, there has been a growing awareness of the potential drug targets for treating a variety of human diseases.[1] The overall strategy in the area of drug discovery has been greatly facilitated by the availability of modern combinatorial and high-throughput facilities.[2] The lead drug compounds, identified by these approaches,[2d-e] are often subject to optimizations by the aids of the structural data of the target macromolecules (mostly enzymes and proteins). However, there is an intrinsic limitation in the structure-based drug design, primarily due to inherent flexibility in the protein structure, as well as the limited geometry of the ligand binding pockets (active sites in the case of enzymes) to accommodate extensive variations in the inhibitor structures.[4] Besides, on the basis of the structural coordinates of the selected enzyme—ligand complexes, it is difficult to predict, a priori, whether the desired changes in the inhibitor
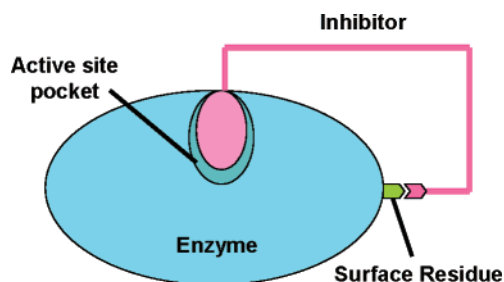

Figure 1. Surface-assisted enhancement in the binding affinity of an inhibitor. The inhibitor is shown to bind at both the active site pocket as well as a surface-exposed residue of an enzyme.

structure would be better accommodated within the active site pockets.[3] However, such limitations could be overcome, at least in principle, by designing enzyme inhibitors, which would not only bind to their cognate enzyme's active site pockets, but also bind (by looping around) to the surface-exposed amino acid residues (Figure 1).

In pursuit of identifying targetable surface-exposed amino acid residues in the vicinity of the enzyme's active site pockets, it was realized that various transition-metal ions (Cu^{2+}, Zn^{2+}, Ni^{2+}) bind to the imidazole group of the histidine residues.[5] The ability of iminodiacetic acid-conjugated Cu^{2+} (IDA-Cu^{2+}) to preferentially interact with the histidine residues of proteins has been utilized to perform the two-dimensional crystallization of proteins at lipid bilayers,[6] purification of peptides and proteins,[7] probing the accessibility of histidine residues,[8] map-

(1) (a) Lindsay M, A. *Nat. Rev. Drug Discovery* **2003**, *2*, 831–838. (b) Hemmila, I. A.; Hurskainen, P. *Drug Discovery Today* **2002**, *7*, 150–156. (C) Stumm, G.; Russ, A.; Nehls, M. *Am. J. PharmacoGenomics* **2002**, *2*, 263–271. (d) Guzey, C.; Spigset, O. *Drug Saf.* **2002**, *25*, 553–560.

(2) (a) Dolle, R. E. *J. Comb. Chem.* **2003** *5*, 693–753. (b) Lee, A.; Breitenbucher, J. G. *Curr. Opin. Drug Discovery Dev.* **2003** *6*, 494–508. (c) Jurinke, C.; van den Boom, D.; Cantor, C. R.; Koster, H. *Adv. Biochem. Eng. Biotechnol.* **2002**, *77*, 57–74. (d) Geysen, H. M.; Schoenen, F.; Wagner, D.; Wagner, R. *Nat. Rev. Drug Discovery* **2003**, *2*, 222–230. (e) Jager, S.; Brand, L.; Eggeling, C. *Curr. Pharm. Biotechnol.* **2003**, *4*, 463–476. (f) Bleicher, K. H.; Bohm, H. J.; Muller, K.; Alanine, A. I. *Nat. Rev. Drug Discovery* **2003**, *2*, 369–378.

(3) (a) Wong, C. F.; McCammon, A. J. *Adv. Protein Chem.* **2003**, *66*, 87–121. (b) Davis, A. M.; Teague, S. J.; Kleywegt, G. J. *Angew. Chem., Int. Ed.* **2003**, *42*, 2718–2736. (c) Neamati, N.; Barchi, J. J., Jr. *Curr. Top. Med. Chem.* **2002**, *2*, 211–227.

(4) (a) Carlson, H. A. *Curr. Opin. Chem. Biol.* **2002**, *6*, 447–452. (b) Wong, C. F.; McCammon, J. A. *Annu. Rev. Pharmacol. Toxicol.* **2003**, *43*, 31–45. (c) Noble, M. E.; Endicott, J. A.; Johnson, L. N. *Science* **2004**, *303*, 1800–1805.

(5) (a) Bal, W.; Christodolou, J.; Sadler, P. J.; Tucker, A. J. *Inorg. Biochem.* **1998**, *70*, 33–39. (b) Sadler, P. J.; Viles. J. H. *Inorg. Biochem.* **1996**, *35*, 4490–4496.

ping the distribution of the histidine residues on the protein surface,[9] and designing inhibitors.[10] Upon a cursory examination of the X-ray crystallographic structures of the enzymes, which are potential targets of drug designing, we found several enzymes containing the surface-exposed histidine residues within $10-15$ Å of the active sites.[11] Of these, carbonic anhydrase was selected as a model system for testing our strategy because of the following reasons: (1) the enzyme has been the target of drug discovery over the last 40 years, for the treatment of a variety of diseases, such as glaucoma, eplipetic seizure, high altitude sickness, and recently for cancer,[10a,12,14] (2) there are 14 different types of isozymes of human carbonic anhydrase, and most of these isozymes have different distribution of the surface-exposed histidine residues,[11e,13] (3) several carbonic anhydrase isozymes have been cloned, expressed, and purified in bulk quantities, and their structural−functional properties have been investigated in considerable detail,[15] and (4) a variety of sulfonamide and hydroxamate derivatives as well as other inhibitors of carbonic anhydrases have been recognized, and their binding affinities have been determined by the kinetic method.[10,14] A preliminary account of our strategy involving the commercially available preparation of bovine carbonic anhydrase (which contained a mixture of carbonic anhydrase isozymes) and a few IDA-Cu^{2+} ligand sulfonamide inhibitors has been recently presented.[10b] To derive quantitative conclusions on the influence of attaching a tether group to benzene-sulfonamide on the enzyme−inhibitor interaction, we designed compound-1 (Figure 2) in the light of the structural coordinates of hCA-II−4-fluorobenzenesulfonamide (FBS) complex (see results) and performed the detailed kinetic and thermodynamic studies.
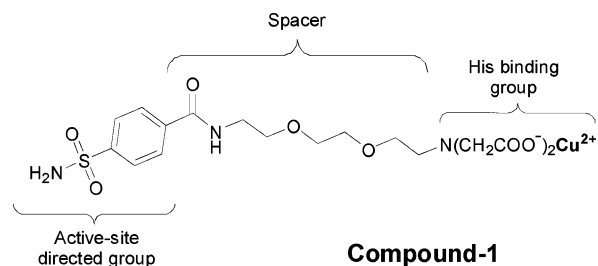

Figure 2. Structure of compound-1. The active site-directed group, benzenesulfonamide, and the histidine binding residue, IDA-Cu^{2+}, are shown to be connected via a triethylene glycol spacer.
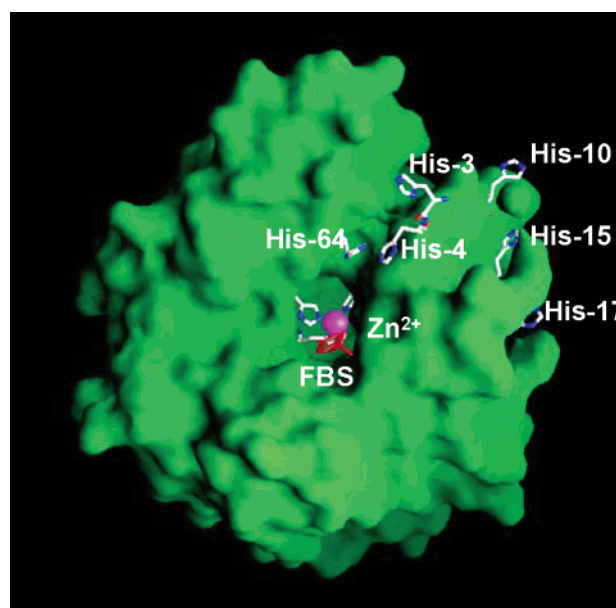

Figure 3. Surface topology of human carbonic anhydrase-II with bound FBS. The surface-exposed histidine residues, the active site Zn^{2+} (surrounded by the histidine residues), and FBS are shown. Generated by the software GRASP.[17]

As will be shown in the subsequent sections, the binding affinity of benzenesulfonamide is enhanced by about 40-fold upon attachment of IDA-Cu^{2+} via the triethylene spacer (compound-1). This quantitative conclusion has been derived both by the steady-state kinetics of the enzyme inhibition data and the direct measurement of enzyme−inhibitor binding affinities. Our overall strategy toward the structure-based design of isozyme-specific inhibitors and the role of the tether group in stabilizing the ground states of the enzyme−inhibitor complexes are discussed in the following sections.

Results

The X-ray crystallographic structure of recombinant human carbonic anhydrase-II (hCA-II) in the presence of FBS (pdb file: 1IF4.pdb) has been known to atomic resolution.[16] The surface topology of the enzyme, its active site binding pocket (containing the histidine-fenced Zn^{2+} and FBS), and the surface-exposed histidine residues are shown in Figure 3.

Note that the N-terminal segment of the enzyme contains six surface-exposed histidine residues, namely His-3, His-4, His-10, His-15, His-17, and His-64. Of these, His-64 has been demonstrated to mediate the proton transfer between exterior solvent molecule and the zinc-bound water at the active site of

(6) (a) Frey, W.; Schief, W. R., Jr.; Pack, D. W.; Chen, C.-T.; Chikotti, A.; Stayton, P.; Vogel, V.; Arnold, F. H. *Proc. Natl. Acad. Sci. U.S.A.* **1996**, *93*, 4937−4941. (b) Pack, D. W.; Chen, G.; Maloney, K. M.; Chen, C. T.; Arnold, F. H. *J. Am. Chem. Soc.* **1997**, *119*, 2479−2487.

(7) (a) Nakagawa, Y.; Yip, T. T.; Belew, M.; Porath, J. *Anal. Biochem.* **1988**, *168*, 75−81. (b) Lanmango, N. S.; Zhu, X.; Lindberg, I. *Arch. Biochem. Biophys.* **1996**, *330*, 238−250. (c) Mrabet, N. T. *Biochemistry* **1992**, *31*, 2690−2702.

(8) Berna, P. P.; Mrabet, N. T.; Van Beeumen, J.; Devreese, B.; Porath, J.; Vijayalakshmi, M. A. *Biochemistry* **1997**, *36*, 6896−905.

(9) Fazal, M. A.; Roy, B. C.; Sun, S.; Mallik, S.; Rodgers, K. R. *J. Am. Chem. Soc.* **2001**, *123*, 6283−6290.

(10) (a) Supuran, C. T.; Scozzafava, A.; Casini, A. *Med. Res. Rev.* **2003**, *23*, 146−189. (b) Roy, B. C.; Hegge, R.; Rosendahl, T.; Jia, X.; Lareau, R.; Mallik, S.; Srivastava, D. K. *J. Chem. Soc., Chem. Commun.* **2003**, 2328− 2329.

(11) (a) Oka, M.; Matsumoto, Y.; Sugiyama, S.; Tsuruta, N.; Matsuhima, M. *J. Med. Chem.* **2000**, *43*, 2479−2483. (b) Phillips, R. S.; Demidkina, T. V.; Faleev, N. G. *Biochim. Biophys. Acta* **2003**, *1647*, 167−172. (c) Pang, S. S.; Guddat, L. W.; Duggleby, R. G. *J. Biol. Chem.* **2003**, *278*, 7639−7644. (d) Qiu, W.; Campbell, R. L.; Gangloff, A.; Dupuis, P.; Boivin, R. P.; Tremblay, M. R.; Poirier, D.; Lin, S. X. *FASEB J.* **2002**, *16*, 1829−1831. (e) Stams, T.; Christianson, D. W. In *The Carbonic Anhydrases: New Horizons*; Chegwidden, W. R., Carter, N. D., Edwards, Y. H., Eds.; Birkhauser Verlag: Basel, 2000; pp 159−174. (f) Vihinen, P. P.; Pyrhonen, S. O.; Kahari, V. M. *Ann Med.* **2003**, *35*, 66−78. (g) Meltzer, H. Y. *J. Clin. Psychiatry* **1991**, *52*, 58−62.

(12) (a) Supuran, C. T. *Expert Opin. Invest. Drugs* **2003**, *12*, 283−287. (b) Rafajova, M.; Zatovicova, M.; Kettmann, R.; Pastorek, J.; Pastorekova, S. *Int. J. Oncol.* **2004**, *24*, 995−1004.

(13) Tureci, O.; Sahin, U.; Vollmar, E.; Siemer, S.; Gottert, E.; Seitz, G.; Parkkila, A.-K.; Shah, G. N.; Grubb, J. H.; Pfreundschuh, M.; Sly, W. S. *Proc. Natl. Acad. Sci. U.S.A.* **1998**, *95*, 7608−7613.

(14) (a) Scozzafava, A.; Owa, T.; Mastrolorenzo, A.; Supuran, C. T. *Curr. Med. Chem.* **2003**, *10*, 925−953. (b) Herker, U.; Pfeiffer, N. *Curr. Opin. Opthalmol.* **2001**, *12*, 88−93. (c) Potter, C. P. S.; Harris, A. L. *Br. J. Cancer* **2003**, *89*, 2−7. (d) Mansoor, U. F.; Zhang, X.-R.; Blackburn, G. M In *The Carbonic Anhydrases: New Horizons*; Chegwidden, W. R., Carter, N. D., Edwards, Y. H., Eds.; Birkhauser Verlag: Basel, 2000; pp 437−459.

(15) (a) Maren, T. H. *Physiol. Rev.* **1967**, *47*, 595−781. (b) Tashian, R. E. *Adv. Genet.* **1992**, *30*, 321−356. (c) Sly, W. S.; Hu, P. Y. *Annu. Rev. Biochem.* **1995**, *64*, 375−401. (d) Tripp, B. C.; Smith, K.; Ferry, J. G. *J. Biol. Chem.* **2001**, *276*, 48615−48618. (e) Schwartz, G. J. *J. Nephrol.* **2002**, *15*, S61− S64.
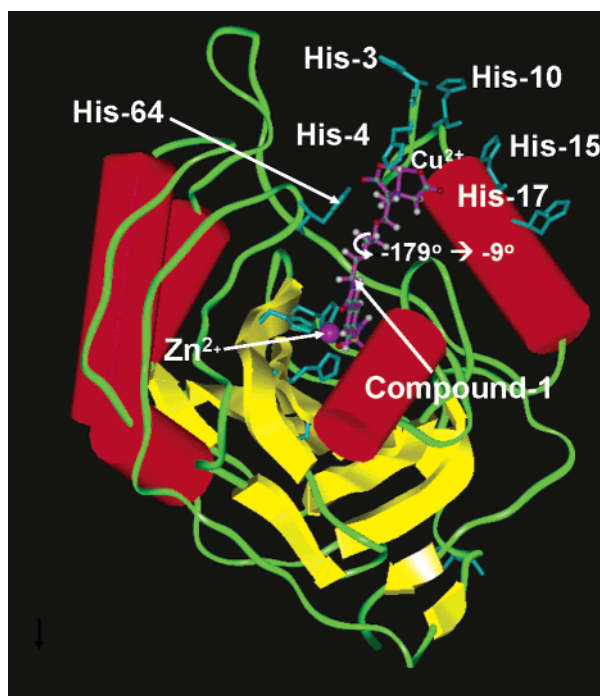
(16) Kim, C.-Y.; Christianson, D. W. PDB file name: 1IF4.pdb.

Figure 4. Structural model of hCAII with modeled compound-1. The bond, which was rotated (from $-179°$ to $-9°$) to position the IDA-conjugated Cu^{2+} in the vicinity of His-4, is highlighted.

the enzyme during catalysis.[18] The linear distance between the active site zinc atom and the NE2 nitrogens of the surface-exposed histidine residues was determined to be 12, 15, 24, 22, 21, and 15 Å for His-64, His-4, His-3, His-17, His-15, and His-10, respectively. In light of these, as well as the location of FBS residue within the enzyme's active site pocket, we decided to attach a triethylene glycol spacer between benzene-sulfonamide and the IDA-Cu^{2+} moieties and synthesize compound-1 (Figure 2). Upon performing the energy minimization of compound-1, it was noted that the distance between the NH_2 nitrogen of benzenesulfonamide and the Cu^{2+} conjugated to the IDA moiety was 19 Å. Hence, it appeared likely that benzene-sulfonamide and IDA-Cu^{2+} moieties of compound-1 would be able to bridge (by small adjustments in the protein and ligand structures) between the active site pocket and one of the surface-exposed histidine residues of the enzyme.

To probe such a possibility, we superimposed the benzene-sulfonamide residue of compound-1 on the known structural coordinate of FBS (bound to hCA-II) and adjusted a few torsional angles while monitoring the steric hindrance ("bump check"). It appeared that just by rotation of the bond between the two methylene groups (next to the amide nitrogen of compound-1) from $-179°$ (original position) to $-9.0°$, the IDA-conjugated Cu^{2+} approached within 2.2 Å distance of the NE2 nitrogen of His-4 (Figure 4). No other surface-exposed histidine residue showed closer proximity (to IDA-Cu^{2+}) than His-4 upon manually adjusting (while maintaining the original position of benzenesulfonamide within the enzyme's active site pocket) other bonds of compound-1. Since the His−Cu^{2+} interaction is

not parametrized in our modeling software, no further attempt was made to energy-minimize the resultant hCA-II-compound-1 structure. However, on the basis of these preliminary modeling data, we have tentatively assigned His-4 as the most likely target for the interaction of IDA-Cu^{2+} of compound-1 (see Discussion section). While we are currently testing the validity of this model by creating the site-specific mutation in His-4 as well as other neighboring residues, we proceeded to ascertain whether the incorporation of IDA-Cu^{2+} to benzenesulfonamide (via the spacer) increased the binding affinity of the parent inhibitor.

Using benzenesulfonamide, compound-1, and Cu^{2+}-depleted compound-1 as the inhibitors, and recombinant human carbonic anhydrase as the enzyme, we performed the steady-state kinetic and ligand binding experiments in 25 mM HEPES buffer, pH 7.0, containing 10% acetonitrile (referred to as the standard HEPES buffer). As detailed in the Experimental Section, the plasmid encoding the full length of human carbonic anhydrase-II was expressed in the *Escherichia coli* BL21 (codon plus DE3 RIL) cells and purified by affinity chromatography on a *p*-aminomethyl benzenesulfonamide-agarose column.[30] The resultant enzyme preparation was judged to be homogeneous by SDS-PAGE. Compound-1 was synthesized by following the protocol outlined in Scheme 1.

Steady-State Kinetic Studies. The time course of the hCA-II-catalyzed reaction was determined by monitoring the hydrolysis of *p*-nitrophenyl acetate at 348 nm.[20] This esterase reaction has been frequently employed for determining the inhibition constants (K_i) of a variety of inhibitors of different carbonic anhydrase isozymes.[21] As noted with other sulfonamide derivatives, compound-1 was also found to serve as a competitive inhibitor of the enzyme against *p*-nitrophenyl acetate as substrate. Figure 5 shows the inhibitor concentration dependence of the initial rates of the hCA-II catalysis in the standard HEPES buffer.

For an easy comparison, the inhibition data are presented as % activity of the enzyme as a function of the total concentration of the inhibitor. Note that as the concentration of the inhibitors increases, the rate of enzyme catalysis decreases. However, such

(17) Nicholls, A.; Sharp, K.; Honig, B. *Proteins: Struct., Funct., Genet.* **1991**, *11*, 281−296.
(18) (a) Tu, C. K.; Silverman, D. N.; Forsman, C.; Jonsson, B. H.; Lindskog, S. *Biochemistry* **1989**, *28*, 7913−7918. (b) Duda, D.; Tu, C.; Qian, M.; Laipis, P.; McKenna, M. A.; Silverman, D. N.; McKena, R. *Biochemistry* **2001**, *40*, 1741−1748.
(19) Roy, B. C.; Mallik, S. *J. Org. Chem.* **1999**, *64*, 2969−2974.
(20) Pocker, Y.; Stone, J. T. *Biochemistry* **1967**, *6*, 668−678.
(21) (a) Forster, R. E. In *The Carbonic Anhydrases: Cellular Physiology and Molecular Genetics*; Dodgson, S. J., Tashian, R. E., Gros, G., Carter, N. D., Eds.; Plenum Press: New York, 1991; pp 79−98. (b) Winum, J.-Y.; Vullo, D.; Casini, A.; Montero, J.-L.; Scozzafava, A.; Supuran, C. T. *J. Med. Chem.* **2003**, *46*, 5471−5477. (c) Vullo, D.; Franchi, M.; Gallori, E.; Antel, J.; Scozzafava, A.; Supuran, C. T. *J. Med. Chem.* **2004**, *47*, 1272−1279.
(22) (a) Chen, R. F.; Kernohan, J. C. *J. Biol. Chem.* **1967**, *242*, 5813−5823. (b) Day, Y. S. N.; Baird, C. L.; Rich, R. L.; Myszka, D. G. *Protein Sci.* **2002**, *11*, 1017−1025. (c) Fierke, C. A.; Calderone, T. L.; Krebs, J. F. *Biochemistry* **1991**, *30*, 11054−11063.
(23) Qin, L.; Srivastava, D. K. *Biochemistry* **1998**, *37*, 3499−3508.
(24) (a) Holm, R. H.; Kennepohl, P.; Solomon, E. I. *Chem. Rev.* **1996**, *96*, 2239−2314. (b) Glusker, J. P.; Katz, A. K.; Bock, C. W. *Rigaku J.* **1999**, *16*, 8−16.
(25) (a) Gray, W. D.; Rauh, C. E. *J. Pharmacol. Exp. Ther.* **1967**, *156*, 383−396. (b) Gray, W. D.; Maren, T. H.; Sisson, G. M.; Smith, F. H. *J. Pharmacol. Exp. Ther.* **1957**, *121*, 160−168. (c) Barnish, I. T.; Cross, P. E.; Dickinson, R. P.; Gadsby, B.; Parry, M. J.; Randall, M. J.; Sinclair, I. W. *J. Med. Chem.* **1980**, *23*, 117−121. (d) Maren, T. H.; Sanyal, G. *Annu. Rev. Pharmacol. Toxicol.* **1983**, *23*, 439−59.
(26) Sharma, S.; Agarwal, G. P. *Anal. Biochem.* **2001**, *288*, 126−140.
(27) Kumar, N. R.; Srivastava, D. K. *Biochemistry* **1995**, *34*, 9434−9443.
(28) Shnek, D. R.; Pack, D. W.; Sasaki, D. Y.; Arnold, F. H. *Langmuir* **1994**, *10*, 2382−2388.
(29) (a) Studier, F.; Rosenberg, A.; Dunn, J.; Dubendorff, J. *Methods Enzymol.* **1990**, *185*, 60−89. (b) Sambrook, J.; Fritsch, E.; Maniatis, T. *Molecular Cloning: A Laboratory Manual*, 2nd ed.; Cold Spring Harbor Laboratory: Cold Spring Harbor, NY, 1989.
(30) Khalifah, R. G. *J. Biol. Chem.* **1971** *246*, 2561−2573.

Scheme 1
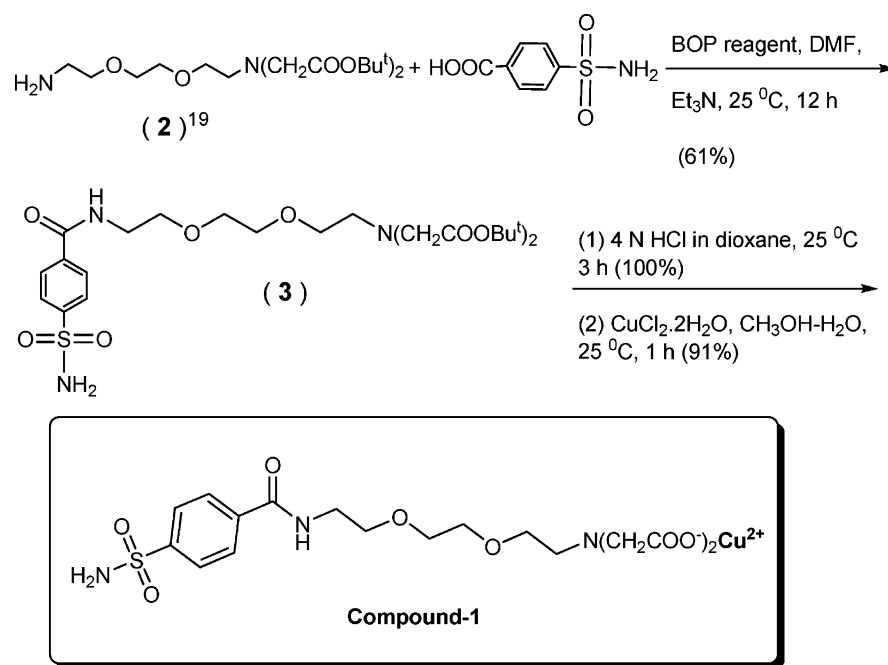
a decrease is considerably steeper with compound-1 (■) than that obtained with the parent compound, benzenesulfonamide (●). These data qualitatively implied that the K_i value of compound-1 was much lower than that of benzenesulfonamide. For quantitative comparison, the data of Figure 5 were analyzed by eq 3. The solid lines are the best fit of the experimental data for the K_i values of sulfonamide and compound-1 being 1.50 μM and 35 nM, respectively. Hence, the incorporation of the tether residue (IDA-Cu^{2+} via the triethylene glycol spacer) to benzenesulfonamide increased the inhibitory potency of compound-1 by about 40-fold.

To further ascertain the contribution of Cu^{2+} vis a vis the remainder of the tether moiety (including IDA and the spacer), we performed the above inhibition studies utilizing Cu^{2+}-depleted compound-1. The data are shown as open triangles in Figure 5. Note a close correspondence between these data and the data for the inhibition of the enzyme by benzenesulfonamide

Figure 5. Steady-state kinetic data for the inhibition of hCA-II. The initial rates of the enzyme-catalyzed hydrolysis of *p*-nitrophenyl acetate substrate were measured as a function of the inhibitor concentrations. [Enzyme] = 1 μM, [*p*-nitrophenyl acetate] = 0.5 mM. The solid smooth lines are the best fits of the data according to eq 3 for the K_i values of benzenesulfonamide (●), compound-1 (■), and Cu^{2+}-depleted compound-1 (△) of 1.5, 35, 1 nM, and 1.5 μM, respectively.

(●). In fact, the fitted line for the benzenesulfonamide-dependent inhibition of the enzyme passes through these data points. Hence, the K_i value for the inhibition of the enzyme by Cu^{2+}-depleted compound-1 has also been taken to be 1.5 μM. These comparative experimental results clearly demonstrate that the enhancement of the inhibitory potency of compound-1 is solely dictated by the presence of Cu^{2+} at the IDA site.

However, on the basis of the above data, we could not rule out the possibility of compensatory effect between different regions of compound-1 (in the absence of Cu^{2+}), yielding the same binding affinity of the Cu^{2+}-depleted compound-1 for hCA-II vis a vis that of benzenesulfonamide. For example, it is possible that triethylene glycol (spacer) and iminodiacetate (chelator) exhibit stabilizing and destabilizing (or vice versa) effects, respectively, and these opposite effects cancel each other. To probe such a possibility, we performed the steady-state kinetic studies for the inhibition of hCA-II, using triethylene glycol-conjugated benzenesulfonamide as an inhibitor. Note that the latter compound is devoid of the iminodiacetate (chelator) moiety. The analysis of the inhibition data (not shown to avoid crowding in Figure 5) by eq 3 produced a K_i value of 0.75 μM for the triethyleneglycol—benzenesuflonamide conjugate. Note that the latter value is only 2-fold lower than that obtained either with benzenesulfonamide or the Cu^{2+}-depleted compound-1. This 2-fold decrease in the K_i value is presumably due to the interaction of triethylene glycol moiety with some group at the enzyme surface. Since iminodiacetic acid does not inhibit hCA-II, we could not perform the above studies. However, if the iminodiacetate moiety of compound-1 exhibits the (opposite) destabilizing effect, its magnitude would, at best, be by 2-fold. Clearly, these effects are not significant as compared to the 40-fold reduction in the K_i value of benzenesulfonamide upon attachment of IDA-Cu^{2+} via the triethylene glycol spacer.

Binding Studies for the Interactions of the Inhibitors to hCA-II. To ensure that the K_i values determined in the previous section were the true measures of the binding affinities of the inhibitors to hCA-II and not due to some unforeseen kinetic
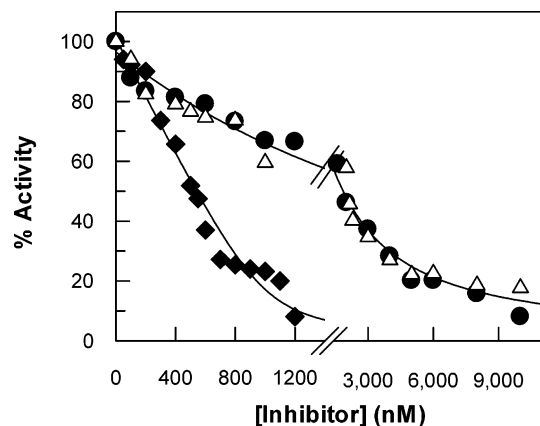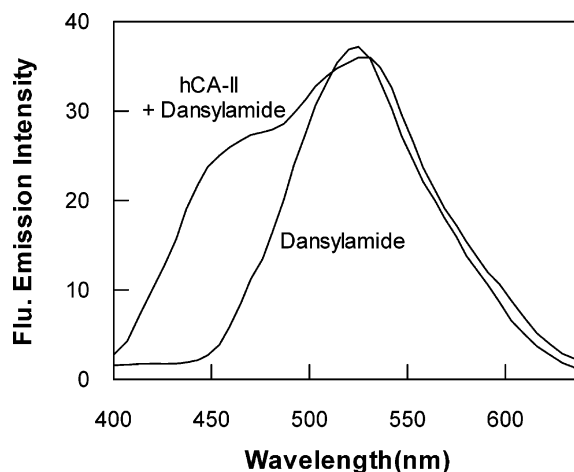
Figure 6. Fluorescence spectra of dansylamide in the absence and presence of hCA-II. [Dansylamide] = 10 μM, [hCA-II] = 1 μM. λ_{ex} = 330 nm.

Figure 7. Binding isotherm of hCA-II−dansylamide complex. The increase in the fluorescence emission intensity at 448 nm (λ_{ex} = 330 nm) for the titration of a fixed concentration of the enzyme (1 μM) with increasing concentrations of dansylamide has been plotted. The solid smooth line is the best fit of the data[23] for the K_d of 3.2 ± 0.24 μM.

Figure 8. Determination of the dissociation constants of the hCA-II−inhibitor complexes by the dansylamide displacement method. (●), (■), and (△) represent the data for benzenesulfonamide, compound-1, and Cu²⁺-depleted compound-1, respectively. [hCA-II] = 1 to 1.1 μM. [Dansylamide] = 10.8 μM. The K_d values of the enzyme−benzenesulfonamide (as well as the Cu²⁺-depleted compound-1) and compound-1 were determined (by the best fit of the data by eq 9) to be 0.66 ± 0.05 μM, and 23.5 ± 3.4 nM, respectively.

complexity, we determined the dissociation constants (K_d) of the enzyme−inhibitor complexes by the dansylamide displacement method.[22] Dansylamide has been known to serve as a fluorogenic ligand for carbonic anhydrases, and it exhibits changes in the fluorescence emission profile upon binding to the enzyme sites. However, since the magnitude of the above spectral changes of dansylamide upon binding to the enzymes (as well as its binding constant) is dependent on the biological origin of the enzyme (including isozymes), buffer composition and its pH, and the stability of dansylamide in the reaction mixture, we acquired the emission spectra of dansylamide in the absence and presence of hCA-II in the standard HEPES buffer. The presence of 10% acetonitrile in our buffer media was found to stabilize the fluorophore during the course of our experiments. Figure 6 shows the fluorescence emission spectra of 10 μM dansylamide (λ_{ex} = 330 nm) in the absence and presence of 1 μM hCA-II. Note that whereas the emission spectrum of free dansylamide shows an emission maximum at 536 nm, the presence of 1 μM enzyme creates a shoulder peak at 448 nm. The change in the fluorescence emission intensity of dansylamide upon binding to hCA-II (at 448 nm) was utilized to determine the dissociation constant of the enzyme−dansylamide complex. Figure 7 shows the titration of a limiting concentration of enzyme by increasing concentrations of dansylamide. Note the increase in fluorescence emission intensity at 448 nm (λ_{ex} = 330 nm) upon increasing the dansylamide concentration.

The binding isotherm was analyzed by a complete solution of the quadratic equation describing the enzyme−ligand interaction, as elaborated by Qin and Srivastava.[23] The solid smooth line is the best fit of the data for the K_d value of the enzyme−dansylamide complex as being equal to 3.2 μM. It should be pointed out the above value is higher than that reported in the literature (0.25−1.2 μM).[22] At this time, we do not understand the origin of this discrepancy.

For determining the dissociation constants of the enzyme−inhibitor complexes, we titrated a fixed concentration of the mixture of the enzyme and dansylamide with increasing concentrations of the inhibitors. The titration data of Figure 8 show that as the concentration of the inhibitor increases, the fluorescence emission intensity (448 nm) of the enzyme−dansylamide complex decreases.
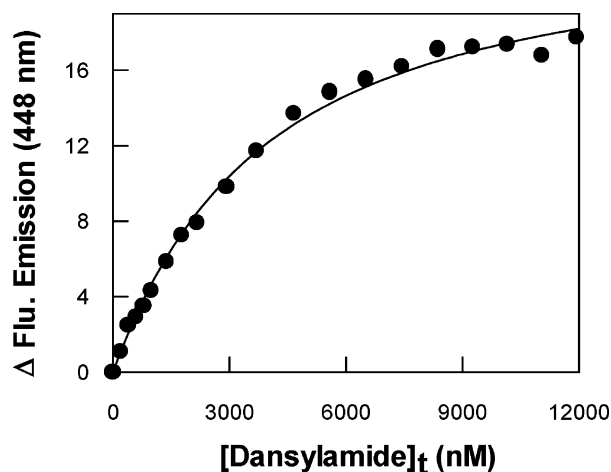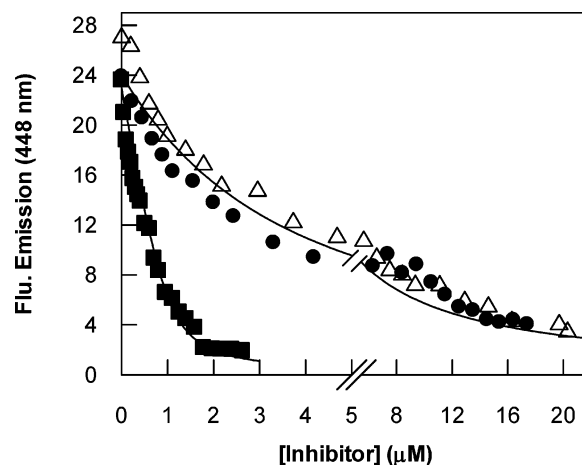
Since the concentrations of some of the inhibitors (e.g., compound-1) were comparable to the concentration of the enzyme, the experimental data were analyzed (solid lines) by a complete solution of the quadratic equation (eqs 8 and 9) for the competitive displacement of the ligands, as described in the Experimental Section. The solid smooth lines are the best fit of the experimental data according to eq 9 for the dissociation constants of the enzyme−benzenesulfonamide (●) and enzyme−compound-1 (■) complexes as being 0.66 μM and 23.5 nM, respectively. Note that these values are similar to the corresponding K_i values (determined by the steady-state kinetic method) of the enzyme−inhibitor complexes. Such a similarity strengthens our deduction that the incorporation of IDA-Cu²⁺ (in conjunction with the tether residue) to benzenesulfonamide indeed enhances the binding affinity of compound-1. To further ascertain the role of Cu²⁺ of compound-1 vis a vis the remainder of the tether chain in enhancing the binding affinity, we performed the above experiment using the Cu²⁺-depleted
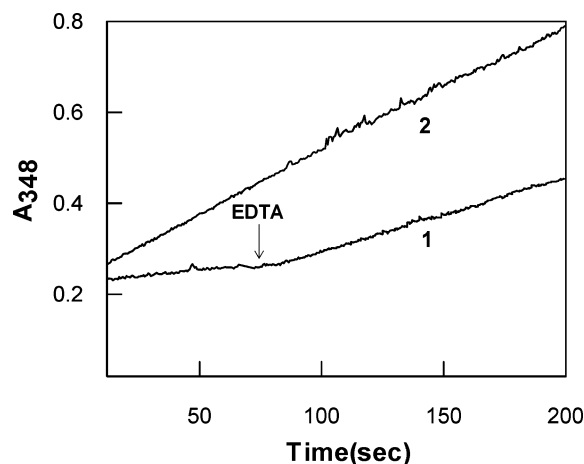
Figure 9. Effect of EDTA on hCA-II-catalyzed reaction in the presence of compound-1. The enzyme-catalyzed hydrolysis of *p*-nitrophenyl acetate in the presence of compound-1, used as such (trace 1) or preincubated with 5 mM EDTA (trace 2). While the reaction was in progress, 5 mM EDTA was added (as shown by arrow) in trace 1. [hCA-II] = 1 μM. [*p*-nitrophenyl acetate] = 0.5 mM. [Compound-1] = 1 μM. The slopes of the trace 1 before and after addition of EDTA were calculated (ΔA_{348}/s) to be 0.0006 and 0.0016, respectively. The slope of trace 2 was calculated to be 0.0028.

compound-1 (Figure 8, $\triangle$). As observed during the K_i measurement (Figure 5), the displacement of the enzyme-bound dansylamide either by benzenesulfonamide or by the Cu^{2+}-depleted compound-1 could be described by a common fitted line for a dissociation constant of 0.65 μM. Hence, in the absence of Cu^{2+}, compound-1 behaves just like benzenesulfonamide, suggesting that the IDA and triethylene glycol spacer do not play any role in stabilizing the enzyme–compound-1 complex.

To ensure that compound-1 served as inhibitor and did not irreversibly inactivate the enzyme, we initiated a steady-state enzyme-catalyzed reaction using *p*-nitrophenyl acetate as a substrate in the presence of compound-1 (Figure 9, trace 1), and a few minutes after the start of the reaction, a small aliquot of EDTA (5 mM) was added. Since EDTA has much higher affinity for Cu^{2+} than IDA,[32] it could easily remove the IDA-bound Cu^{2+}. As shown in Figure 9 (trace 1), as soon as EDTA is added to the reaction mixture, the time course of the reaction progress increases sharply. The rate of the latter process was found to be about 3-fold faster than that observed prior to the addition of EDTA. When we performed the above steady-state experiment utilizing EDTA-incubated compound-1, the initial rate of the enzyme catalysis was found to be faster than that observed without EDTA. These qualitative experiments clearly rule out the possibility of inactivation of hCA-II in the presence of compound-1.

Discussion

The strategy of enhancing the binding affinities of the active site-directed inhibitors by incorporating IDA-Cu^{2+} moieties via suitable spacers is expected to find a variety of applications in pharmaceutical, agricultural, and biotechnological industries. Such applications may range from the de novo designing of highly potent and isozyme-specific inhibitors such as potential drugs, insecticide, and herbicide agents, designing compounds

that would promote and/or preclude protein–protein, protein–lipid, protein–carbohydrate, and protein–nucleic acid interactions, crystallization of membrane-bound proteins, etc. However, to successfully employ this methodology, the following criteria must be met: (1) The targetable enzyme structures must have their surface-exposed residues (potential of interacting with Cu^{2+}) within 15–25 Å from the active site-directed ligands. (2) The active site pockets of the enzymes must *not* be buried deep into the protein structures. (3) The inhibitory features must be desirable at or near the neutral pH. The latter is particularly so since at higher pH, Cu^{2+} interacts with different side chain groups of proteins.[6]

Various transition-metal ions are known to interact with different types of organic compounds, including the amino acid side chain groups of proteins.[24] However, the molecular mechanism of protein–metal interaction is very complex and is contributed by a combination of electrostatic, hydrophobic, and/or donor–acceptor (coordination) factors.[26] The overall energetics of one type of interaction versus the other is dictated by the nature of chelating ligand, metal ion, surface amino acid composition, and the surrounding chemical environment (e.g., pH, ionic strength, etc.). However, on the basis of a variety of the affinity chromatography data, it has been argued that at neutral pH, the binding of proteins to IDA-Cu^{2+} columns is generally limited to metal coordination by surface-accessible histidine residues.[6] At higher pH values, other basic groups of amino acid side chains (or N-terminus group) can interact with IDA-Cu^{2+}. Since the imidazole group of histidine has a pK_a of 6.8, it serves as an ideal ligand for interaction with IDA-Cu^{2+} at neutral pH. By using the diethylpyrocarbonate modified proteins, Arnold and her collaborators have shown (via the ESR spectroscopy) that the native proteins are targeted to IDA-Cu^{2+} lipid assemblies through coordination by surface histidines.[28] However, there are reports of involvement of other amino acid side chains (e.g., Trp, Phe, Tyr, Cys) of proteins in binding to metal affinity columns, but the mechanism of such interaction is not yet clear.[26]

Although the above discussion suggests that IDA-Cu^{2+} moiety of compound-1 has potential to interact with the surface-exposed histidine (presumably His-4 as discerned via the modeling studies) of hCA-II, we cannot rule out the possibility of involvement of the thiol group of cysteine and the indole nitrogen of tryptophan in such interactions. Although there is no surface-exposed cysteine residue in hCA-II, there are two surface-exposed tryptophans (Trp-5 and Trp-16) in the vicinity of the histidine clusters near the N-terminal end of hCA-II. We are currently in the process of performing the site-specific mutations of different N-terminal histidine (as well as tryptophan) residues in hCA-II to ascertain their contributions in binding to IDA-Cu^{2+}, and we will report these findings subsequently.

However, one of the major advantages of the imidazole–IDA-Cu^{2+} interaction is its prevalence in the aqueous medium.[24] This is presumably because in aqueous solution, the IDA-conjugated Cu^{2+} contains a bound water molecule, which is exchanged by the interaction of the lone pair electrons of the nitrogen of the imidazole residues (pK_a = 6.8), forming a stable Lewis acid–base pair. Hence, unlike other polar amino acid side chains of proteins, the histidine–Cu^{2+} interaction does not involve high energetic costs for desolvating the interacting

(31) Dill, K. A. *J. Biol. Chem.* **1997** 272, 701–704.
(32) Sillen, L. G.; Martell, A. E. In *Stability Constants of Metal Ion Complexes*, 2nd ed.; The Chemical Society: London, 1964.

species. Evidently, targeting the surface-exposed histidines may emerge to be an energetically facile strategy in the inhibitor designing endeavors. A casual perusal of the X-ray crystallographic structures in the Brookhaven Protein Data Bank reveals that several enzymes, which are the potential targets of drug/herbicide designs, contain the surface-exposed histidines in the vicinity of their active site pockets. These enzymes include 17β-hydroxysterioid dehydrogenase, (target for breast cancer), tyrosinase (target for cutaneous melanoma),[11f] adenylate kinase (target for neurological disorder),[11g] aldose reductase (target for diabetes),[11a] and acetolactate synthase (target for the herbicide design).[11c] The binding affinities of the putative inhibitors of these enzymes can be significantly enhanced by attaching Cu^{2+}-conjugated tether residues (to the active site-directed inhibitors), which would interact with one of the surface-exposed histidine residues of the enzymes.

It should be mentioned that the length of spacers between the active site-directed and IDA-Cu^{2+} moieties need not be precise in designing the inhibitors to bridge between the active site and surface-exposed histidine residues in enzymes. This is presumably because of the inherent flexibility in the enzyme structures as well as the adjustments in inhibitor structures. Although the above features have entropic disadvantage, the latter is compensated by the enthalpic gain due to the IDA-Cu^{2+}–histidine interaction. For example, while designing compound-1, we selected triethylene glycol as spacer just to provide an approximate length so that benzenesulfonamide could bind to the active site and the IDA-Cu^{2+} could bind to His-4. Our recent isothermal titration microcalorimetric data reveal that the enthalpic changes of compound-1 is much higher than those accounted for the binding of individual moieties. On the other hand, the free-energy changes of compound-1 is less than those envisaged for the "additive" effect[31] (our unpublished results).

The other advantage of using the surface-exposed histidine residues as the second anchor site is the possibility of designing isozyme-specific inhibitors. For example, because of the marked similarity in the active site geometry of different carbonic anhydrase isozymes,[11e] benzenesulfonamide cannot serve as an ideal drug for inhibiting one isozyme (e.g., hCA-II) without affecting the others. This is why several sulfonamide inhibitors, initially approved as the anticonvulsants, cerebral vasodilators, diuretics, and antiglaucoma agents, were subsequently withdrawn from the market because of serious side effects.[25] Since the surface distribution of the histidine residues are different among different carbonic anhydrase isozymes, it is highly plausible to achieve the isozyme selectivity by employing our "two-prong" approach in inhibitor designing.

From the mechanistic point of view, the experimental data presented in the previous section clearly demonstrates that the incorporation of IDA-Cu^{2+} to benzenesulfonamide via triethylene glycol enhances the binding affinity of the parent compound by about 40-fold. This has been demonstrated by both the comparative steady-state kinetic and the ligand displacement method. The fact that the above enhancement in the binding affinity is primarily contributed by the presence of Cu^{2+} at the IDA site comes from the experiments involving Cu^{2+}-depleted compound-1 (see Figures 5 and 8). The binding affinity of Cu^{2+}-depleted compound-1 exhibits nearly the same affinity for hCA-II as that of benzenesulfonamide, and there is no major compensatory effect for the binding of triethylene

glycol spacer and IDA groups in the absence of Cu^{2+}. This suggests that neither IDA nor triethylene glycol spacer has any additive contribution in stabilizing the ground state of the enzyme–inhibitor complex.

Experimental Section

Materials. Zinc sulfate, ampicillin, chloramphenicol, and IPTG were purchased from Life Science Resources, Milwaukee, WI. Yeast extracts and tryptone were purchased from Becton Dickinson, Sparks, MD. Acetonitrile was purchased from Aldrich Chemical Co., Milwaukee, WI. HEPES, *p*-aminomethylbenzenesulfonamide-agarose, *p*-nitrophenyl acetate, and PMSF were obtained from Sigma, St. Louis, MO. Dansylamide was purchased from Avocado Research Chemicals, Heysham, Lancs, U.K. All the chemicals needed for synthesis of compound-1 were purchased from Aldrich Chemical. The expression cells BL21 codon plus DE3(RIL) were from Stratagene, La Jolla, CA. All other chemicals were of reagent grade and were used without further purification.

Methods. Synthesis of Compound-1. To a suspension of 4-carboxybenzenesulfonamide (280 mg, 1.39 mmol) in dichloromethane (13 mL) and triethylamine (0.7 mL, 5 mmol), DMF (5 mL) was added to make a solution. BOP reagent (616 mg, 1.39 mmol) was added to it, followed by the addition of **2**[19] (575 mg, 1.52 mmol) in dichloromethane (2 mL). The reaction was continued for 12 h at room temperature with stirring and then quenched with a saturated aqueous solution of NaCl. The aqueous phase was extracted with ethyl acetate. The combined organic layer was washed successively with 5% citric acid, water, 5% $NaHCO_3$, and water. The organic layer was dried over Na_2SO_4 and evaporated under reduced pressure to provide the crude product as a viscous liquid. The crude product was purified by column chromatography (silica gel, initially with dichloromethane, and then 5% methanol in dichloromethane) to give **3** as a viscous oil, 520 mg (61%). ^1H NMR (CDCl$_3$, 300 MHz): δ 1.45 (s, 18H), 2.64 (d, 2H, $J = 9$ Hz), 2.88 (s, 2H), 2.96 (s, 2H), 3.39 (s, 2H), 3.48–3.72 (m, 8H), 6.14 (br, 1H), 7.71–8.01 (m, 4H).

Compound **3** (305 mg, 0.54 mmol) was taken in a solution of 4 N HCl in 1,4 dioxane (6 mL) and was stirred for 5 h at room temperature. The solvents were removed by rotary evaporator, and the residue was dried under vacuum. The desired acid was obtained as the HCl salt (263 mg, 99%) and used as such for the next step without further purification. ^1H NMR (DMSO-d_6, 500 MHz): δ 3.41–3.52 (m, 9H), 3.59–3.75 (m, 3H), 4.17 (s, 4H), 7.49 (br, 2H), 7.87 (d, 2H, $J = 10$ Hz), 8.0 (d, 2H, $J = 10$ Hz). ^{13}C NMR (DMSO-d_6, 125 MHz): δ 55.41, 65.97, 69.41, 69.86, 70.18, 126.28, 128.56, 137.86, 146.88, 165.95, 168.21.

Acid sulfonamide (130 mg, 0.27 mmol) was dissolved in MeOH (6 mL), and an aqueous solution of saturated $NaHCO_3$ (1 mL) was added. Solid $CuCl_2\cdot2H_2O$ (45.8 mg, 0.27 mmol) was then added with stirring. Immediate precipitation took place. The reaction mixture was stirred for 30 min at room temperature. The solvents were evaporated to dryness under reduced pressure. The residue was dissolved in a minimum quantity of water, and MeOH was added to it, causing precipitation. The precipitate was filtered, again dissolved in a minimum quantity of water, and precipitated by absolute ethanol. Filtration of the precipitate and drying under vacuum provided the pure **compound-1** as a blue solid; 130 mg (91%). Anal. Calcd For $C_{17}H_{23}CuN_3O_9S\cdot H_2O$: C, 38.74; H, 4.78; N, 7.97. Found: C, 39.03; H, 4.64; N, 7.68.

Expression and Purification of the Recombinant Human Carbonic Anhydrase-II. The expression vector pMA-5-8 containing human carbonic anhydrase-II gene (at the Sma I and BamH I restriction cleavage sites) was obtained as a gift from Dr. Carol Fierke's laboratory. The plasmid was transformed into *E. coli* BL21 codon plusDE3(RIL) host cells by following the standard molecular biology protocol.[29] The transformed cells were grown in LB medium, supplemented with 100

μg of ampicillin/mL, 50 μg/mL of chloramphenicol, and 60 μg/mL of ZnSO$_4$ at 37 °C until A_{600} was 0.6. The expression of hCA-II was induced by addition of 400 μM IPTG and 400 μM ZnSO$_4$. The cells were incubated further at 25 °C overnight. The cells were centrifuged at 5000g for 15 min. The pellet was washed in 20 mM Tris-HCl, pH 8.7, and resuspended in the same buffer containing 0.5 mM EDTA. A working concentration of 1 mM PMSF in 2-propanol was added prior to sonication. The cells were sonicated for a total time of 10 min in a Branson bath sonifier utilizing 40% duty cycle in an ice cold bath. The sonicated extract was centrifuged at 15 000 rpm for 30 min, and the supernatant (crude extract) was collected for further purification.

The enzyme activity of the recombinant human carbonic anhydrase II was measured in 25 mM HEPES buffer, pH 7.0, containing 10% acetonitrile (the standard buffer) at 25 °C, utilizing 0.4 mM *p*-nitrophenyl acetate as substrate.[20] The protein concentration was determined according to the Bradford method, utilizing BSA as the standard protein.

The recombinant form of human carbonic anhydrase II was purified from the crude extract using *p*-aminomethyl benzenesulfonamide-agarose column.[30] The enzyme concentrations were determined spectrophotometrically using $\epsilon_{280} = 54$ mM^{-1} cm^{-1} based on MW = 30 000. The purified enzyme was subjected to the SDS-PAGE analysis to confirm the homogeneity of the enzyme.

Steady-State Kinetics for the Inhibition of hCA-II. The steady-state kinetic experiments for the hCA-II catalyzed reaction were performed on Perkin-Elmer Lambda 3B spectrophotometer. All the steady-state experiments were performed in the standard HEPES buffer containing 10% acetonitrile. The latter solvent ensured the solubility of the substrate during the course of the reaction, and it did not exhibit any influence on the catalytic activity of the enzyme. The initial rates of the enzyme-catalyzed reactions were measured by following the hydrolysis of the chromogenic substrate, *p*-nitrophenyl acetate, at 348 nm.[20]

The steady-state kinetic experiments were performed in a total reaction volume of 1.3 mL (in the standard buffer), containing 0.5 mM *p*-nitrophenylacetate and varied concentrations of the inhibitors. The initial rates of the enzyme catalysis were determined by taking the slopes of the reaction traces. For easy comparison of the inhibition data, the initial rates were translated into % activity as a function of the inhibitor concentrations.

Because of slow esterase activity of hCA-II, fairly high concentration of the enzyme (∼1 μM) is utilized to reliably measure the initial rates of the enzyme reaction at 348 nm. With such a high concentration of the enzyme, part of the substrate and/or inhibitor can be envisaged to be bound to the enzyme site. Since the Michaelis−Menten equation relies on the free rather than the total concentrations of the substrates and inhibitors, the fraction of the bound species must be subtracted from their total concentrations for analyzing the kinetic data. For the hCA-II catalyzed esterase reaction, the above constraint is not a major problem since the K_m for *p*-nitrophenyl acetate is about 4 mM, and as long as the substrate concentration is maintained in the range of 1 mM or higher, the total concentration of the substrate could be taken as the measure of the free concentration. However, this would not be the case with tight binding inhibitors (K_i in the range of nM). Hence, for inhibitors, the free concentrations must be calculated from the total concentration by complete solution of the quadratic equation describing enzyme−inhibitor interaction. Equation 1 is a classic steady-state equation for the competitive inhibition of the enzyme.

$$v = \frac{V_{max}}{1 + K_m/[S]\,(1 + [I]_f/K_i)} \qquad (1)$$

where $[I]_f$ is the free concentration of the inhibitor. If by experimental design the substrate concentration can be maintained considerably lower than the K_m value ($[S]_{total} \ll K_m$), eq 1 can be further simplified to the form of eq 2. In fact, the above condition is an obligatory requirement

for the hCA-II-catalyzed esterase reaction, since the *p*-nitrophenyl acetate is not very soluble in the reaction buffer.

$$v = \frac{V_{max}*[S]/K_m}{1 + [I]_f/K_i} \qquad (2)$$

In the absence of any inhibitor, the numerator term of eq 1 can be taken as the measure of v_0 (the initial velocity of the enzyme-catalyzed reaction in the absence of inhibitor). Besides, $[I]_f$ can be represented in the form of total concentration of the enzyme and inhibitor by a complete solution of the quadratic equation describing their interaction. With these solutions, the final form of the competitive steady-state model can be given by eq 3.

$$v = \frac{v_0*K_i}{K_i + ([I]_t - 0.5\{([I]_t + [E]_t + K_i) - \sqrt{([I]_t + [E]_t + K_i)^2 - 4*[I]_t*[E]_t}\})} \qquad (3)$$

The inhibition data of Figure 5 have been analyzed by eq 3 using the nonlinear regression analysis software Grafit 4.0.

Spectrofluorometric Studies. All the spectrofluorometric studies involving dansylamide were performed on Perkin-Elmer Lambda 50-B spectrofluorometer equipped with a magnetic stirrer and thermostated water bath. To ensure the stability of dansylamide during the course of the titration as well as kinetic experiments, its stock solution (1 mM) was prepared in 10 mM HCl, and it was diluted in the standard HEPES buffer containing 10% acetonitrile. The emission spectra of dansylamide in the absence and presence of hCA-II were acquired by fixing the excitation wavelength at 330 nm, and both excitation and emission slits were maintained at 5 mm with a cutoff filter at 390 nm.

The dissociation constant of the hCA-II−dansylamide complex was determined by titrating a fixed concentration of the enzyme (1 μM) with increasing concentrations of dansylamide in the standard HEPES buffer, pH 7.0, containing 10% acetonitrile. The initial reaction volume was 2.0 mL. The excitation and emission wavelengths were maintained at 330 and 448 nm with a cutoff filter at 390 nm. The excitation and emission slits were 5 mm each. The dissociation constant of the enzyme−dansylamide complex was determined by analyzing the binding isotherm as described by Qin and Srivastava.[23]

The dissociation constant of the hCA-II−inhibitor complex was determined by competitive displacement of a fixed concentration of dansylamide by increasing concentrations of the inhibitor. In a typical experiment, an equilibration mixture containing 1 μM hCA-II and 10 μM dansylamide in the standard HEPES buffer (pH 7.0, containing 10% acetonitrile) was titrated with increasing concentrations of the inhibitor. The initial reaction volume was 2.0 mL, and the reaction content was continuously stirred during the course of the titration. The excitation and emission wavelengths were maintained at 330 and 448 nm, respectively, with a cutoff filter at 390 nm. The excitation and emission slits were 5 mm each. Since the binding of the inhibitor competitively displaced dansylamide from the enzyme site, the fluorescence intensity at 448 nm decreased, and the data were analyzed by a modified form of the competitive binding model as elaborated by Kumar and Srivastava.[27]

If two ligands (e.g., dansylamide and benzenesulfonamide, represented by D and B, respectively) compete for an enzyme site (E), it is intuitively obvious that the dissociation constant for the EB complex can be determined if the dissociation constant of ED complex is already known. Such a determination would be relatively easy if $[E]_{total} \ll K_d$ (D) and K_d (B), and $[E]_{total} \ll [D]_{total}$ and $[B]_{total}$. Under this situation, the total concentrations of ligands can be taken as being equal to their free concentrations. On the other hand, if this ideal situation is not satisfied and the enzyme−ligand dissociation constants are comparable to the initial concentrations of the enzyme and ligands (such as encountered in the fluorescence titration data of Figure 8), the

dissociation constant determination of one enzyme−ligand complex by the competitive displacement method becomes cumbersome. However, recourse can be made if the dissociation constant of the one-enzyme ligand complex is relatively higher than that of the other, as observed for the binding of dansylamide versus compound-1 to the hCA-II site. The competitive binding of dansylamide (D) versus benzenesulfonamide (B) to the hCA-II (E) site can be formalistically represented by eq 4.

$$
\begin{array}{c}
E + D \underset{K_d}{\overset{\longrightarrow}{\rightleftharpoons}} ED \\
+ \\
B \\
K_b \Updownarrow \\
EB
\end{array}
\qquad (4)
$$
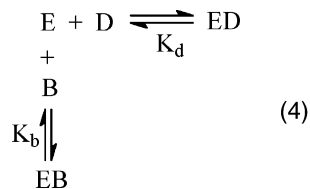
In eq 4, K_d and K_b are the dissociation constants of the hCA-II−dansylamide (ED) and hCA-II−benzenesulfonamide (EB) complexes, respectively. If the free and total concentrations of E, D, and B are represented by [E], [D], and [B] and $[E]_t$, $[D]_t$, and $[B]_t$, respectively, K_d and K_b can be represented as follows.

$$K_d = [E][D]/[ED] = [E]([D]_t - [ED])/[ED] \qquad (5)$$

$$K_b = [E][B]/[EB] = [E]([B]_t - [EB])/[EB] \qquad (6)$$

If $[E]_t \ll [D]_t$, then $[D]_t$ can be taken to be the measure of [D], and by taking into account the mass balance ($[E]_t = [E] + [ED] + [EB]$), $[E]_t$ can be represented by eq 7.

$$[E]_t = [EB] + \frac{K_b[EB]}{[B]_t - [EB]} + \frac{K_b[EB][D]}{([B]_t - [EB])K_d} \qquad (7)$$

Equation 7 can be simplified to yield the dependence of [EB] on the concentrations and the binding constants of other species (eq 8).

$$[EB] = ([E]_t + [B_t + K_b + (K_b/K_d)[D]_t) - \frac{\sqrt{([E]_t + [B_t + K_b + (K_b/K_d)[D]_t)^2 - 4[E]_t[B]_t}}{2} \qquad (8)$$

The dissociation constant of the enzyme−inhibitor complex is determined by monitoring the decrease in the fluorescence of the enzyme-dansylmide complex ($\lambda_{ex} = 330$ nm, $\lambda_{em} = 448$ nm) as a function of increasing concentration of the inhibitor. Hence, the observed fluorescence (F_{obsd}) as a function of the inhibitor ([B]) concentration can be given by eq 9

$$F_{obsd} = \Delta F_{max}/[E]_t * ([E]_t - [EB]) \qquad (9)$$

where ΔF_{max} is the maximum change in fluorescence upon complete displacement of dansylamide from the enzyme site. The titration data of Figure 8 were fitted by the nonlinear regression analysis of eq 9 using the software package Grafit 4.

Molecular Modeling Studies. The molecular modeling studies were performed on a Silicon Graphics-O2 molecular modeling workstation with the aids of Accelrys softwares, InsightII(98), Discover, and biopolymers. The coordinates for the X-ray crystallographic structures of human carbonic anhydrase-II complexed with FBS (PDB file: 1IF4.pdb) were downloaded from the Brookhaven Protein Data Bank. The structure of compound-1 was first subjected to energy minimization by the aid of Discover. The sulfonamide ring of compound-1 was manually superimposed on the enzyme-bound structural coordinate of FBS. This was followed by manually adjusting the torsion angles of different single bonds of the spacer moiety, while measuring the distance between the Cu^{2+} (bound to IDA) and the surface-exposed histidine residues. It was noted that just by rotating the bond between two methylene group (as shown in Figure 4) from its original angle of $-179.7°$ to $-9.0°$, the IDA-bound Cu^{2+} reached closest (2.2 Å away) to His-4.

Conclusions

The present article provides a novel strategy for enhancing the binding affinity of an active site-directed inhibitor by attaching an iminodiacetic acid (IDA)-conjugated Cu^{2+} (via triethylene glycol as spacer), which could interact with one of the surface-exposed histidine (His-4) residues. Although the overall approach has been developed for human carbonic anhydrase-II, the overall strategy can be adopted for designing highly potent inhibitors for other pathogenic enzymes as potential drugs. Since the surface residues are unlikely to be conserved during the course of the natural selection process, our contemplated approach has the potential to generate isozyme-specific inhibitors for selected enzymes.